




ORIGINAL ARTICLE

Iron isotope fractionation in soil and graminaceous crops after 100 years of liming in the long-term agricultural experimental site at Berlin-Dahlem, Germany

Bei Wu¹  | Yi Wang¹  | Anne E. Berns¹ | Kathlin Schweitzer² | Sara L. Bauke³  | Roland Bol¹ | Wulf Amelung^{1,3}

¹Institute of Bio- and Geosciences: Agrosphere (IBG-3), Forschungszentrum Jülich GmbH, Jülich, Germany

²Department of Crop and Animal Sciences, Humboldt-Universität zu Berlin, Berlin, Germany

³Institute of Crop Science and Resource Conservation, Soil Science and Soil Ecology, University of Bonn, Bonn, Germany

Correspondence

Bei Wu, Institute of Bio- and Geosciences: Agrosphere (IBG-3), Forschungszentrum Jülich GmbH, Wilhelm-Johnen-Straße, 52428 Jülich, Germany.
Email: b.wu@fz-juelich.de

Funding information

Bundesministerium für Bildung und Forschung, Grant/Award Number: 031B0026C

Abstract

Sustainable arable cropping relies on repeated liming. Yet, the associated increase in soil pH can reduce the availability of iron (Fe) to plants. We hypothesized that repeated liming, but not pedogenic processes such as lessivage (i.e., translocation of clay particles), alters the Fe cycle in Luvisol soil, thereby affecting Fe isotope composition in soils and crops. Hence, we analysed Fe concentrations and isotope compositions in soil profiles and winter rye from the long-term agricultural experimental site in Berlin-Dahlem, Germany, where a controlled liming trial with three field replicates per treatment has been conducted on Albic Luvisols since 1923. Heterogeneity in sub-soil was observed at this site for Fe concentration but not for Fe isotope composition. Lessivage had not affected Fe isotope composition in the soil profiles. The results also showed that almost 100 years of liming lowered the concentration of the HCl-extractable Fe that was potentially available for plant uptake in the surface soil (0–15 cm) from 1.03 (standard error (*SE*) 0.03) to 0.94 (*SE* 0.01) g kg⁻¹. This HCl-extractable Fe pool contained isotopically lighter Fe ($\delta^{56}\text{Fe} = -0.05$ to -0.29%) than the bulk soil ($\delta^{56}\text{Fe} = -0.08$ to 0.08%). However, its Fe isotope composition was not altered by the long-term lime application. Liming resulted in relatively lower Fe concentrations in the roots of winter rye. In addition, liming led to a heavier Fe isotope composition of the whole plants compared with those grown in the non-limed plots ($\delta^{56}\text{Fe}_{\text{WholePlant}_+ \text{Lime}} = -0.12\%$, *SE* 0.03 vs. $\delta^{56}\text{Fe}_{\text{WholePlant}_- \text{Lime}} = -0.21\%$, *SE* 0.01). This suggests that the elevated soil pH (increased by one unit due to liming) promoted the Fe uptake strategy through complexation of Fe(III) from the rhizosphere, which favoured heavier Fe isotopes. Overall, the present study showed that liming and a related increase in pH did not affect the Fe isotope

This is an open access article under the terms of the Creative Commons Attribution License, which permits use, distribution and reproduction in any medium, provided the original work is properly cited.

© 2020 The Authors. European Journal of Soil Science published by John Wiley & Sons Ltd on behalf of British Society of Soil Science.

compositions of the soil, but may influence the Fe isotope composition of plants grown in the soil if they alter their Fe uptake strategy upon the change of Fe availability.

Highlights

- Fe concentrations and stocks, but not Fe isotope compositions, were more heterogeneous in subsoil than in topsoil.
- Translocation of clay minerals did not result in Fe isotope fractionation in the soil profile of a Luvisol.
- Liming decreased Fe availability in topsoil, but did not affect its $\delta^{56}\text{Fe}$ values.
- Uptake of heavier Fe isotopes by graminaceous crops was more pronounced at elevated pH.

KEYWORDS

liming, plant-available Fe pool in soil, winter rye, $\delta^{56}\text{Fe}$

1 | INTRODUCTION

As an essential nutrient, iron (Fe) is involved in numerous physiological processes, such as respiration, photosynthesis and DNA biosynthesis (Kappler & Straub, 2005; Marschner, 1995; Weber et al., 2006). Bioavailable Fe(II) is rapidly oxidized to Fe(III) in the presence of oxygen and subsequently forms Fe(III) (hydr)oxides, the solubility of which drastically decreases with increasing pH (Blume et al., 2016). Particularly in calcareous soils, severe Fe deficiency in plants may occur due to poor Fe availability under these pH conditions (Chen & Barak, 1982). In agricultural production systems, Fe availability may be reduced due to liming that is needed to maintain soil structure, to balance soil acidity, to optimize the supply of other essential nutrients such as P, and to replenish base metal nutrients (i.e., calcium (Ca) and magnesium (Mg)) (Bolan et al., 2003; Haynes & Naidu, 1998). Over-application of lime may cause plants to take up Fe in a non-physiological form, leading to Fe deficiency in plants (lime-induced chlorosis) (e.g., Blume et al., 2016; Fageria et al., 1995).

Plants acquire Fe from the rhizosphere either through reduction or complexation strategies, so-called strategy I and II, respectively. Uptake strategy II is mainly used by graminaceous plants, including important staple crops such as rice, wheat and barley, by secreting phyto-siderophores from their roots and forming Fe(III)-phytosiderophore complexes to improve Fe solubility in the rhizosphere (Mori, 1999; Shojima et al., 1990). However, Fe use by plants may not be restricted to one uptake strategy. Recent studies indicate that strategy I plants can also secrete Fe-binding compounds (e.g., Fourcroy et al., 2014), whereas functional Fe(II) transporters have also been found in rice (Ishimaru et al., 2006). In any case, both Fe uptake into, and translocation and transformation

within, plants can result in Fe isotope fractionation, the extent of which can be different in graminaceous and non-graminaceous plants (e.g., Guelke-Stelling & von Blanckenburg, 2012; Kiczka et al., 2010). Non-graminaceous plants, utilizing the reduction strategy, tend to take up lighter Fe isotopes that are preferentially released during reductive dissolution of Fe-containing minerals in soil (Wiederhold et al., 2006; see also Wu et al., 2019 for a review). Kiczka et al. (2010) illustrated how Fe isotope fractionation might take place in non-graminaceous plants. However, mechanisms of Fe isotope fractionation in graminaceous plants still remain unclear owing to inconsistent fractionation effects described among the limited number of studies (Wu et al., 2019; see also Figure SI1). Kiczka et al. (2010) and Guelke-Stelling and von Blanckenburg (2012) argued that the Fe isotopic signature of a plant did not only depend on the Fe uptake strategy, but also on the nutrient availability in the growth substrate. This statement was only recently confirmed by a study where rice plants showed different Fe isotope compositions when growing under Fe-sufficient or Fe-deficient conditions (Liu et al., 2019). However, evidence of varying Fe isotope compositions upon different Fe availabilities is still needed to better understand Fe isotope fractionation in other graminaceous plants.

In the present study, we sampled soils and graminaceous crops (winter rye) at the long-term agricultural experimental site in Berlin-Dahlem, Germany, which had received liming treatments for almost 100 years (Krzysch et al., 1992). The soil at the studied site was an Albic Luvisol, for which we analysed Fe isotope compositions of the soil profiles down to the depth of 100 cm to test the hypothesis (1) that physical clay illuviation during pedogenesis has not altered Fe isotope

composition in the soil. In addition, we studied the HCl-extractable Fe pool to test the hypothesis (2) that long-term liming practices would affect Fe pools that are potentially available for plant uptake. Finally, we analysed Fe concentrations and isotope compositions of the winter rye plants grown in limed and non-limed plots to test the hypothesis (3) that Fe uptake by the crop plants would be altered due to changed soil conditions after liming, which would eventually be reflected by Fe isotope signatures of the crop grown in the limed soil.

2 | MATERIALS AND METHODS

2.1 | Site, sampling and sample pretreatment

The soils and plants were sampled at the long-term Static Soil Use Experiment (BDa_D3) in Berlin-Dahlem, Germany (52°28'02"N, 13°17'49"E) (Figure S2, detailed site description can be found in the Supporting Information section, and in Krzysch et al., 1992). The soils were characterized as Albic Luvisols according to the World Reference Base (IUSS Working Group WRB, 2015). Liming has been performed since 1923 to study its effect on soil and crop performance (Krzysch et al., 1992). Dolomitic lime was applied in spring 2014 and 2016 at a rate of 250 kg CaO ha⁻¹ a⁻¹. In the limed plots (+L1, +L2 and +L3) the soil pH was generally about one unit higher than in the three plots without lime application (−L1, −L2 and −L3) (Figure S3). The crop at the sampling time was winter rye (*Secale cereale* L.).

The soil sampling took place in April 2016 before renewed liming. Two soil cores were taken at diagonally opposing corners of each plots down to 100-cm depth with a soil auger of 6-cm inner diameter, which was lined with an inner plastic sleeve for sample recovery (Walter et al., 2016). The soil cores were divided into six segments, representing the depths of 0–15, 15–30, 30–40, 40–50, 50–70 and 70–100 cm, respectively. The corresponding soil core segments of the two cores taken in one plot were well mixed on site and subsampled for the present study. In each plot, at least 10 winter rye plants were sampled at the flowering stage in May 2017 and separated into roots, stems, leaves and spikes. In total, there were 18 soil samples (i.e., six soil segments × three field replicates) and 12 plant samples (four organs × three field replicates) for each treatment (i.e., lime or no lime).

2.2 | Sample preparation

Total concentrations of Fe (Fe_{Total}) and other major elements in soil were analysed after digestion of 0.05 g soil

with 0.25 g lithium meta/tetraborate at 1050°C for 3 hr. For the purpose of Fe isotope study, pressurized microwave-assisted digestion (turboWAVE, Milestone Srl, Sorisole, Italy) was applied to digest soils in a mixture of concentrated HNO₃ and H₂O₂, which released about 80–100% of total Fe (Figure S4), termed bulk Fe (Fe_{Bulk}). The Fe pool in the soil potentially available to plants was extracted by 0.5 M HCl for 24 hr (Fe_{HCl}), as this method did not induce Fe isotope fractionation during extraction (Guelke et al., 2010; Wiederhold et al., 2007). Kiczka et al. (2011) showed that HCl might also dissolve Fe in silicate minerals that was not readily available to plants. In this regard, we termed this pool as “HCl-extractable Fe” instead of the “plant-available Fe pool” in the following sections. Iron in winter rye organs was also extracted by the pressurized microwave-assisted digestion.

2.3 | Iron purification and isotope analysis

Separation of Fe from matrix elements in the sample was performed in a customer-designed laminar flow box in a cleanroom at the Agrosphere Institute at Forschungszentrum Jülich GmbH, using anion exchange chromatography resin (Bio-Rad AG1-X4, 200–400 mesh, Munich, Germany) following the published method of Dauphas et al., 2004. Iron isotope analysis was performed on multi-collector inductively coupled plasma mass spectrometer (MC-ICP-MS, Nu Plasma II, Nu Instruments Ltd, Wrexham, UK) coupled with a desolvating nebulizer system (Aridus II, Teledyne Cetac, Omaha, USA) in high mass resolution mode with a mass resolving power (Rp_{5,95%}) of >8,000 at ion beam transmission of 10%. To correct instrumental mass bias, a strategy of standard-sample-standard bracketing was applied using IRMM-524a with a matched Fe concentration (500 ppb) to the samples.

2.4 | Data calculation and statistics

The results of Fe isotope analysis in samples were expressed using IRMM-014 as the standard (recommended by Dauphas et al., 2017), as follows:

$$\delta^{56}\text{Fe}(\text{‰}) = \left(\frac{\frac{{}^{56}\text{Fe}_{\text{sample}}}{{}^{54}\text{Fe}_{\text{sample}}}}{\frac{{}^{56}\text{Fe}_{\text{IRMM-014}}}{{}^{54}\text{Fe}_{\text{IRMM-014}}}} - 1 \right) * 1000$$

Long-term external precision was achieved at 0.08‰ and 0.12‰ for δ⁵⁶Fe and δ⁵⁷Fe, respectively, based on two times the standard deviation (SD) of the δ⁵⁶Fe values

of the repeated measurement of the IRMM-524a during the analytical sessions. The three-isotope plot (Figure S5) indicated the absence of mass-independent fractionation during the analyses. The analyses were validated by repeated and in-laboratory cross-checked measurements of the in-house standard for soil (Luvisol, collected at Klein-Altendorf Experimental Station (50°37'9" N, 6°59'29" E) of the University of Bonn, Germany) and the NIST SRM 1575a (Table S1).

Statistical analyses were performed using OriginPro (V. b9.2.272; OriginLab, 2015). The significance of differences in Fe concentration and isotope composition between samples from limed and non-limed plots ($n = 3$ for each treatment) was assessed by performing two-sample t -test following an F -test for testing equality of variances, whereas the differences between topsoil and subsoil, among plant organs, or between plants and the HCl-extractable Fe pool of respective treatments ($n = 3$ for each variant) were evaluated by paired-sample t -test. Significance of differences was accepted at $p < .05$. If a significant difference occurred, we performed the least-significant-difference (LSD) procedure. Detailed Materials

and Methods can be found in the Supporting Information section.

3 | RESULTS

3.1 | Iron concentration, stock and isotope composition in bulk soil

Total Fe concentrations in the topsoil (0–30 cm) of both limed and non-limed plots were found to be similar and showed little spatial variation (Figures 1a, S6a). In contrast, Fe concentrations in subsoil varied among plots, especially in the soil core segments between the ploughing depth and 70 cm, with a large range from about 5 to 20 g kg⁻¹ (Figure S6a), reflecting heterogeneous material deposition during the last ice age (Chmielewski & Köhn, 1999). Only two plots (+L2 and +L3) were alike in their Fe concentrations at every depth. The smallest Fe concentrations below 40 cm were found in plot –L2, where the subsoil contained more silt and less clay than in the other plots (Hobley & Prater, 2019).

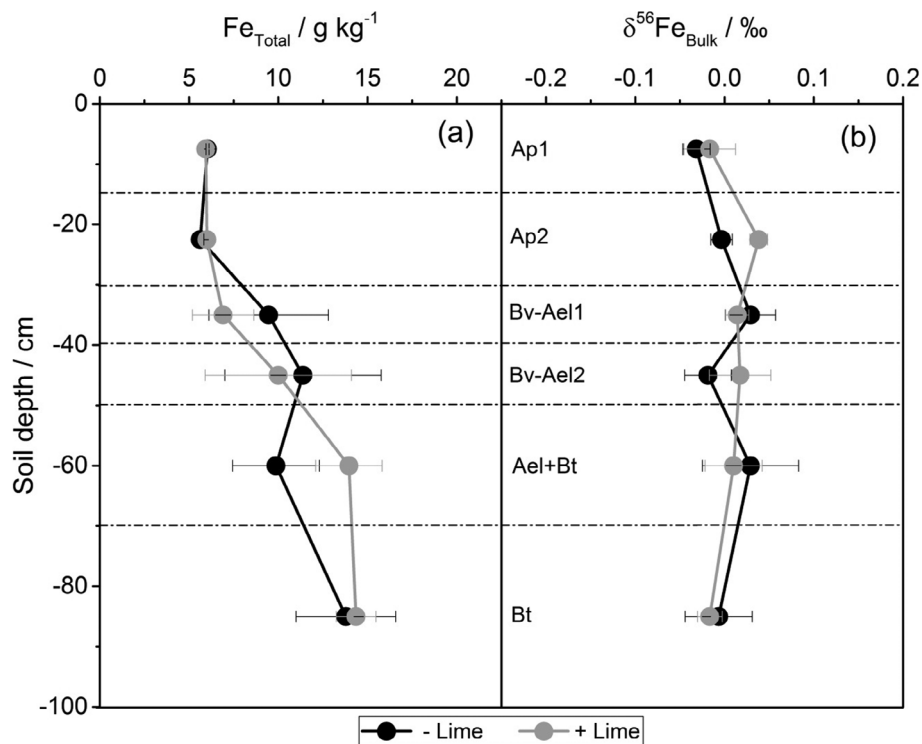


FIGURE 1 Depth profiles of total Fe concentrations (a) and isotope compositions (b) of the bulk soil at the long-term experimental field in Berlin-Dahlem. The horizontal dashed lines indicate the analysed soil core segments. The soil horizons are German descriptions of a representative key soil profile at the experimental site, where Ap is the ploughed topsoil, Bv-Ael and Ael correspond to an eluvial horizon, and Ael + Bt and Bt to an argic horizon according to World Reference Base (IUSS Working Group WRB, 2015). The bars are standard error of the mean of three field replicates for no-lime (black) and lime (grey) management, respectively, showing heterogeneity of subsoil, but not of the topsoil, with respect to Fe content. The studied Luvisol exhibited relatively uniform Fe isotope compositions. Values between limed and non-limed plots were not statistically significant at the $p = .05$ level of probability

Correspondingly, total Fe stocks varied in the subsoil, with the mean values of 1.86×10^5 (standard error (*SE*) 0.33×10^5) and 1.76×10^5 (*SE* 0.38×10^5) kg ha^{-1} for limed and non-limed plots (Figure 2), respectively, without significant difference between the two treatments.

The Fe isotope compositions within the soil profiles down to 100 cm ($\delta^{56}\text{Fe}_{\text{Profile}}$) were 0.00‰ (*SE* 0.03) and 0.00‰ (*SE* 0.01) for the bulk soil of the limed and non-limed plots, respectively (Figure 1b), identical within error between the treatments and to the representative parent material (+0.01‰, 2SD 0.05, analytical error, $n = 4$, see Supplementary Information for parent material collection). The lateral difference in $\delta^{56}\text{Fe}$ values within the same soil segment across the fields ($\leq 0.16\text{‰}$) was comparable to the vertical difference within a soil profile ($\leq 0.13\text{‰}$) (Table S2, Figure S7a).

3.2 | HCl-extractable Fe pool in soil

The extraction by diluted HCl (Fe_{HCl}) targets the so-called plant-available Fe pool (Guelke et al., 2010), which includes water-soluble Fe, exchangeable Fe, organically sorbed/bound Fe and short-range-ordered Fe minerals (Wiederhold et al., 2007). Our soil profiles contained 10–19% of total Fe (Fe_{Total}) in the form of HCl-extractable

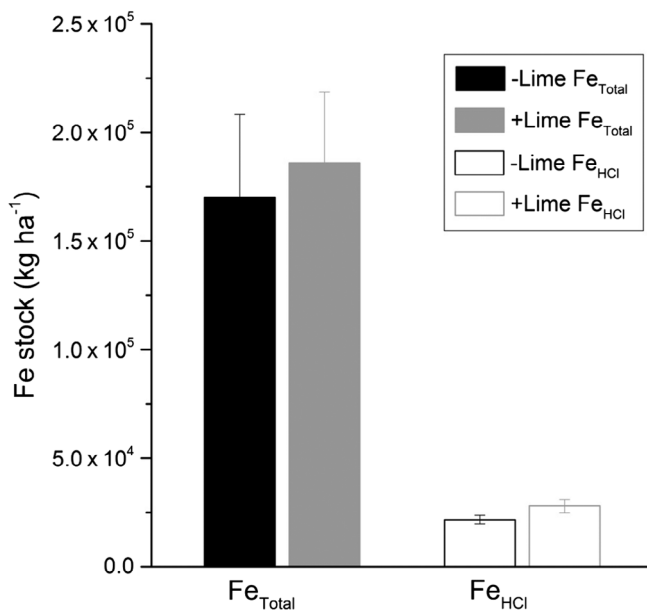


FIGURE 2 Iron stocks of the total Fe pool (Fe_{Total}) and the HCl-extractable Fe pool (Fe_{HCl}) in the limed (grey) and non-limed (black) plots within the soil depth of 0–100 cm. The bars are standard error of the mean of three field replicates for no-lime (black) and lime (grey) management, respectively. Values between limed and non-limed plots were not statistically significant ($p = .05$)

Fe (Fe_{HCl}) (Figure S6b,c). The topsoil contained larger Fe_{HCl} fractions relative to the Fe_{Total} pool compared with the subsoil. Similar to the bulk soil, the Fe concentrations in the Fe_{HCl} pool were relatively homogeneous in the topsoil and heterogeneous in the subsoil (Figures 3a, S6b). The Fe_{HCl} concentration in the surface soil (0–15 cm) treated with lime was significantly less than in the non-limed treatment (LSD = 0.070 < difference of the means 0.092). In addition, greater Fe_{HCl} stocks in the soil down to 100 cm (Figure 2) were found in the limed plots, although the difference between the limed and non-limed plots was not statistically significant ($p = .16$).

The Fe_{HCl} pool was isotopically lighter than Fe in bulk soil (Figures 3b, S7). The differences in $\delta^{56}\text{Fe}$ values between the Fe_{HCl} pool and the bulk soil, expressed as $\Delta^{56}\text{Fe}_{\text{HCl-Bulk}}$, ranged from -0.04 to -0.39‰ (Table S2). Unlike the limited isotope fractionation of the bulk soil profiles, the Fe isotope compositions of the Fe_{HCl} pool ($\delta^{56}\text{Fe}_{\text{HCl}}$) showed a decreasing pattern from -0.09‰ (*SE* of the mean of all six plots 0.01) in the topsoil (0–30 cm) to -0.23‰ (*SE* of the mean of all six plots 0.02) at 100-cm depth. The highest $\delta^{56}\text{Fe}_{\text{HCl}}$ values appeared in the soil core segment of 15–30 cm for both limed and non-limed fields. The Fe isotope compositions of the Fe_{HCl} pool did not vary significantly in limed and non-limed plots.

3.3 | Iron concentration and isotope composition in winter rye

The Fe concentrations of winter rye roots tended to be less when grown in the limed plots than those in the non-limed plots (Figure 3a, S7), although the differences were not statistically significant across the field replicates ($p = .10$). Compared with the Fe_{HCl} pool in the topsoil (0–30 cm), the variations of Fe concentrations in the plant roots were considerably larger (coefficient of variation 0.14 vs. 0.03 and 0.30 vs. 0.06 for limed and non-limed treatments, respectively). Aboveground organs contained much smaller Fe concentrations than the roots, with the stems containing the least Fe per kg dry mass (Figure 3a).

In spite of the large variations of the Fe concentrations, the Fe isotope compositions in the roots were within a narrow range and did not differ between the plants grown in the soils with or without lime application (-0.02‰ , *SE* 0.03 vs. -0.04‰ , *SE* 0.02; Figures 3b, S8, Table S3). In contrast, aboveground organs exhibited variable Fe isotope compositions ranging from -0.30 to -0.83‰ , which was much lighter than those in the roots. Compared with the Fe_{HCl} pool of the topsoil where the roots were mainly located, the roots of winter rye presented similar or slightly heavier Fe isotope compositions,

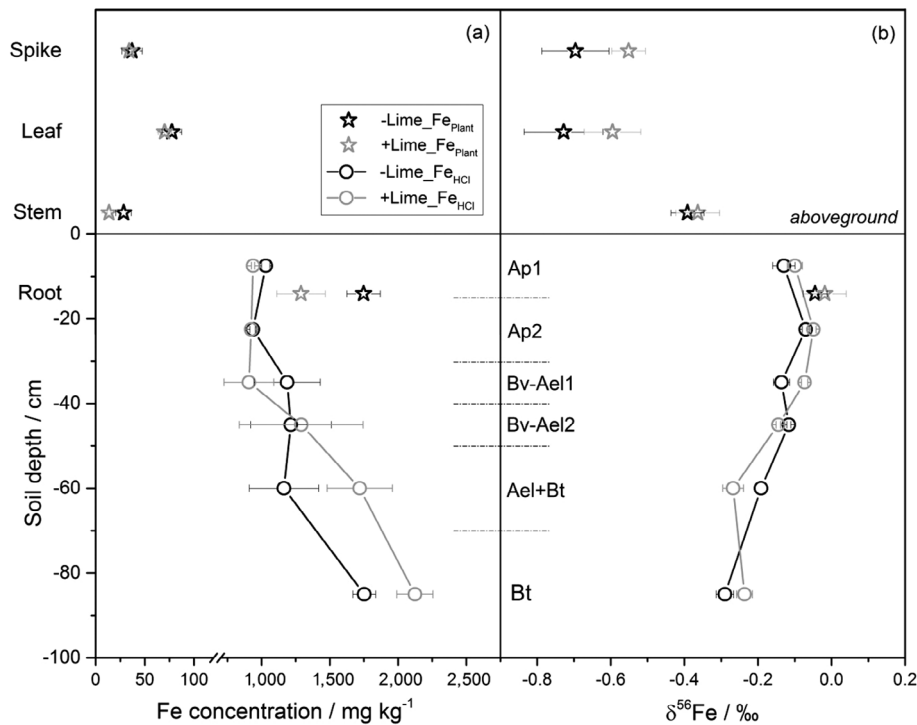


FIGURE 3 Iron concentrations (a) and isotope compositions (b) of the Fe_{HCl} pool representing the plant-available Fe in the soil core segments (circle) and of the organs of winter rye (Fe_{Plant} , star), showing that most Fe was accumulated in the roots of winter rye, which exhibited the heaviest Fe isotope composition compared with either the aboveground organs or the Fe_{HCl} pool in the soil where they had grown. Winter rye plants grown in limed plots showed heavier Fe isotope compositions ($\delta^{56}\text{Fe}_{\text{WholePlant}_{\text{+Lime}}} = -0.12\text{‰}$, $SE\ 0.03$) than those grown in non-limed plots ($\delta^{56}\text{Fe}_{\text{WholePlant}_{\text{-Lime}}} = -0.21\text{‰}$, $SE\ 0.01$). Values between limed and non-limed plots were not statistically significant ($p = .05$), except for the Fe concentrations in the Fe_{HCl} pool in the 0–15-cm soil layer. The short horizontal dashed lines indicate the analysed soil core segments. The soil horizons are German descriptions of a representative key soil profile at the experimental site, where Ap is the ploughed topsoil, Bv-Ael and Ael correspond to an eluvial horizon, and Ael + Bt and Bt to an argic horizon according to World Reference Base (IUSS Working Group WRB, 2015). The bars are standard error of the mean of three field replicates for no-lime (black) and lime (grey) management, respectively. Note that the plant tissues are not positioned on the true scale of their heights

with $\Delta^{56}\text{Fe}_{\text{Root-HCl}}$ values of 0.06 ($SE\ 0.04$) and 0.05 ($SE\ 0.03$) for limed and non-limed plots, respectively. It is noteworthy that the aboveground organs of winter rye, especially the leaves and the spikes, were enriched in relatively heavier Fe isotopes when grown in limed soil than those taken from the control plots without lime (Figure 3b), although the differences were not statistically significant ($p = .16$ for leaves and $p = .07$ for spikes).

4 | DISCUSSION

4.1 | Total Fe and HCl-extractable Fe pools in the studied Luvisol

Previous studies showed that pedogenic processes can fractionate Fe isotopes in soil relative to the parent material, with resulting changes in $\delta^{56}\text{Fe}$ values from -0.52 to $+0.72\text{‰}$ in the studied soil profiles to date (Wu et al., 2019). Under reducing conditions (e.g., Gleysols)

dissolution of primary Fe-minerals preferentially releases isotopically light Fe(II) into solution, leaving a weathered residue enriched in heavy Fe isotopes, whereas the light Fe isotopes are translocated within the soil profile or exported laterally. However, under permanent oxidizing conditions or moderate soil weathering (e.g., Cambisols) Fe isotope fractionation can be limited throughout the soil profile. In addition, eluviation and illuviation processes can result in Fe-depleted and Fe-enriched zones with significant differences in Fe isotope compositions (e.g., Podzols). Albic Luvisols as studied here are characterized by significant lessivage, that is, the downward migration of clay particles in the field. However, this process did not induce significant Fe isotope fractionation, as each of the studied profiles showed relatively homogeneous Fe isotope compositions within the soil profiles, with vertical variations of $\delta^{56}\text{Fe}$ values $\leq 0.13\text{‰}$. The lack of Fe isotope fractionation clearly supported the theory of lessivage, indicating a physical mobilization of colloids, for instance, after snowmelt, or a simple physicochemical

release of colloids at low ionic strength after moderate acidification (e.g., Rousseau et al., 2004; Ryan & Gschwend, 1998). Our results demonstrated that the processes occurring in these soils did not necessarily involve significant chemical alteration of Fe pools, in contrast to those observed, for example, during redox processes or podzolization in soils (Wu et al., 2019).

The investigated Luvisol received low precipitation (annual precipitation of 562 mm) and no waterlogging was observed during sampling due to the sandy texture. Aerobic conditions thus prevailed in the soil. The lack of stagnant water prevented a profound reductive dissolution of Fe-containing minerals, which would preferentially mobilize light Fe isotopes (Crosby et al., 2005; Crosby et al., 2007; Wiederhold et al., 2006; Wu et al., 2019). In combination with the limited vertical water transport due to low precipitation amounts, no significant Fe isotope fractionation was observed in the studied soil profiles. These relatively uniform Fe isotope compositions throughout the profiles were in line with other aerobic soils studied in temperate climates, such as Cambisols, for example, in France, Germany, Switzerland and Canada, without pronounced redoximorphic features (Fekiacova et al., 2013; Wiederhold et al., 2007).

The Fe pool extracted by diluted HCl (Fe_{HCl}) was suggested to be potentially available to plant uptake (Guelke et al., 2010). The contribution of organically sorbed/bound Fe to the Fe_{HCl} pool was low, as the soil was poor in organic matter (0.06–0.71%). In addition, water-extractable Fe could also be neglected in such an aerobic soil with limited amounts of drainage water. We, therefore, suspect that the Fe_{HCl} fraction consisted largely of short-range-ordered Fe minerals in our soil. The subsoil contained similar or larger concentrations of HCl-extractable Fe, reflecting its release from overall larger total Fe stocks compared with the topsoil. However, the utilization of subsoil Fe by plants depends not only on its pool size, but largely also on its availability and accessibility to plants, which is usually much lower than in the surface soil due to its higher bulk density, lower air permeability, higher physical resistance for the root, and lower contents of organic matter and microbial biomass, which all contribute to overall limitations in root growth and nutrient uptake (Blume et al., 2016; Kautz et al., 2013).

In contrast to the bulk soil, the Fe_{HCl} pool was characterized by a light Fe isotope signature, probably due to isotopically lighter Fe in short-range-ordered Fe minerals formed after preferential dissolution of light Fe isotopes followed by immediate precipitation in the presence of oxygen (see review by Wu et al., 2019). The vertical profiles of the $\delta^{56}\text{Fe}$ values of the Fe_{HCl} pool indicated a stronger depletion of heavy Fe isotopes in the deeper soil

layers of both limed and non-limed plots, along with increasing amounts of extracted short-range-ordered Fe minerals. In addition, compared with the subsoil, the topsoil was much more influenced by the plants. The harvest and removal of isotopically light aboveground organs, as well as the accumulation of the roots with relatively heavier Fe isotope composition in the topsoil, might also result in the topsoil becoming isotopically heavier over years compared with the subsoil.

Long-term liming resulted in an increase of pH on average by one unit (Figure S3). This indicates that Fe speciation in the soil might vary, and thus Fe isotope composition of the soil might also change (Lotfi-Kalahroodi et al., 2019). However, neither the Fe isotope compositions of the total Fe pools nor those of the HCl-extractable Fe pools were significantly affected by liming (Figures 1, 3b). We attribute this to the larger unchanged Fe pools compared with those altered by pH.

4.2 | Iron accumulation and isotope fractionation in winter rye

As a graminaceous crop, winter rye is likely to utilize the complexation strategy (i.e., strategy II) upon Fe deficiency, in which phytosiderophores are released from the plant root to mobilize Fe(III) compounds by complexation of Fe(III) and formation of Fe(III)-phytosiderophores in order to acquire Fe from the rhizosphere (Marschner et al., 1986). In our field, Fe deficiency symptoms were not observed and the crops produced similar yields in both limed and non-limed plots in the year of sampling in the field (Figure S9). This indicates that Fe was not a limiting factor at our site, even after long-term liming practice. However, we observed that the roots of winter rye in one of the limed plots (+L3) contained only about half the concentration of Fe compared with the plants of other plots. This finding indicates that Fe availability was considerably different in plot +L3 from that in the other plots (Ågren & Weih, 2012), although Fe concentrations of the Fe_{HCl} pool were similar among the plough layers of the plots. In addition, the plants grown in the limed plots tended to be enriched in heavier Fe isotopes compared with their counterparts growing in the non-limed plots ($\delta^{56}\text{Fe}_{\text{WholePlant}} - 0.12\text{‰}$, $SE\ 0.03$ vs. -0.21‰ , $SE\ 0.01$, based on mass balance calculation, see Supplementary Information), suggesting that elevated pH due to liming favoured the uptake of heavy Fe isotopes.

In this regard, Fe isotope composition of the plants relative to the growth media (here assumed to be the Fe_{HCl} pool) may provide some information about the dominant Fe uptake strategy that the plants have

utilized. When strategy I is used reduction of Fe(III) to Fe(II) in the rhizosphere would result in isotopically light Fe(II) being taken into the plant, leading to an enrichment of light Fe isotopes in the root epidermis and inner root tissues (and eventually the whole plant). On the other hand, complexation induces less Fe isotope fractionation (e.g., equilibrium fractionation between inorganic aqueous Fe(III) and Fe(III)-siderophore $\sim 0.6\%$ in $\delta^{56}\text{Fe}$; Dideriksen et al., 2008) than reduction (e.g., equilibrium fractionation between aqueous Fe(III) and Fe(II) $\sim 3\%$ in $\delta^{56}\text{Fe}$; Johnson et al., 2002). The Fe isotope composition of the whole plant would then only marginally differ from that of the plant-available Fe in the growth substrate. Iron isotope fractionation due to the uptake through complexation of Fe(III) would then depend on the variation of isotope compositions between different Fe(III) species in the rhizosphere and in the root epidermis. This phenomenon of varied isotope fractionation effects was observed for rice (Liu et al., 2019), which can utilize both Fe(III) and Fe(II) from the rhizosphere (Ishimaru et al., 2006). At our site, the difference between the Fe isotope compositions of the whole plant and the Fe_{HCl} pool ($\Delta^{56}\text{Fe}_{\text{WholePlant-HCl_Topsoil}}$) was only marginal. We, therefore, suggest that as typical for graminaceous plants, strategy II was the dominant pathway of Fe uptake in winter rye growing in our field, even though no symptoms of Fe deficiency were observed. However, we could not fully rule out the contributions of uptake strategy I for Fe acquisition, as the extent of Fe isotope fractionation by either of the two different strategies is still uncertain. Under liming conditions, where the soil pH increased by one unit (Figure S3), the reduction of Fe(III) becomes less effective due to the fact that the pH may be beyond the optimum of the ferric chelate reductase present in the root epidermis (Morrissey & Guerinot, 2009). In contrast, the transport of Fe(III)-phytosiderophores can still be efficient at elevated pH through the complexation strategy (Schaaf et al., 2004). Therefore, winter rye might more likely utilize strategy II for Fe uptake at higher pH, leading to relatively heavier Fe isotope compositions of the plants than those growing without lime (Table S3). However, to be able to use the Fe isotope composition as a tracer to elucidate Fe uptake by plants, further studies are needed on how and to what extent Fe isotope fractionation takes place in plants under different nutrient conditions.

Aboveground organs of winter rye were enriched in light Fe isotopes with a $\Delta^{56}\text{Fe}_{\text{Shoot-Root}}$ value of -0.50% (SE 0.07 of samples from all the six plots). We attribute this difference to the variation of Fe speciation during in-plant translocation and redistribution. To reach the xylem from the root epidermis, Fe is symplasmically transported in the form of Fe(III)-deoxymugineic acid or

other forms of Fe(III)-phytosiderophores (Nozoye et al., 2011). In the xylem, Fe(III)-citrate is present in both non-graminaceous and graminaceous plants, whereas in graminaceous plants, additional Fe(III)-phytosiderophores are predominant (Ariga et al., 2014). This indicates that from the root epidermis to the xylem of graminaceous plants, Fe can always be present in its ferric forms and reduction of Fe(III) to Fe(II) probably does not occur. Therefore, Fe isotope compositions of the tissues would vary mainly owing to the change of the binding ligands and their respective abundance in the tissue. Morgan et al., (2010) showed a strong positive correlation between measured Fe isotope fractionation factors and the Fe-binding affinities of chelating ligands. In addition, Fe(III)-phytosiderophores have been shown to be about 1.5% heavier in $\delta^{56}\text{Fe}$ than Fe(III)-citrate (Moynier et al., 2013). This suggests that the xylem can exhibit a lighter Fe isotope composition than the root epidermis or the cortex, because the xylem can contain a mixture of Fe(III)-phytosiderophores and isotopically lighter Fe(III)-citrate, whereas the root epidermis accumulates isotopically heavier Fe(III)-phytosiderophores. Driven by transpiration and root pressure, Fe is transported upwards in the xylem to aboveground organs, with the productive organs and younger leaves importing additional Fe from the phloem (Curie et al., 2009).

Unlike in the xylem, Fe in the phloem is mainly chelated with nicotianamine and deoxymugineic acid (Kato et al., 2010; Nishiyama et al., 2012). As nicotianamine has a higher affinity to Fe(III) but forms the more stable Fe(II)-nicotianamine complex, the phloem sap may consist of a mixture of Fe(II) and Fe(III) species with a variation of up to 3% in $\delta^{56}\text{Fe}$ between the two species (Moynier et al., 2013). Hence, the phloem sap may exhibit a lighter Fe isotope signature compared with the xylem sap. The isotopically light Fe pool in the phloem is further transported into younger leaves and flowers/seeds and then stored in seeds in its Fe(III) forms (e.g., Briat, 1999; Ravet et al., 2008; Vazzola et al., 2007). Younger organs are usually found to be enriched in light Fe isotopes, as suggested by Kiczka et al. (2010) and Guelke-Stelling and von Blanckenburg (2012). However, heavier Fe isotope compositions in seeds compared with other organs have also been observed (e.g., Arnold et al., 2015; Moynier et al., 2013, Figure S1). Our data showed that the Fe isotope compositions of the spikes of winter rye were similar to those of the leaves but lighter than those of the stems. The variable difference in Fe isotope signatures between seeds and straws among plant species is likely to be because seeds receive Fe either via xylem vessels or via the sieve tubes of the phloem, as both circulate around the seed coat (Grillet et al., 2014). The contribution of each Fe pathway varies among plant species

depending on the presence of xylem discontinuity at the base of seeds, especially those of cereal crops, as demonstrated for Zn by Stomph et al. (2009). In addition, we observed that, despite the fact that each analysed plant sample was a pooled sample of several individual plants, the $\delta^{56}\text{Fe}$ values of the same aboveground organs from the same treatment still differed by up to 0.2‰ (in leaves and spikes). We could thus conclude that the variation of Fe isotope composition of individual plants can even be larger, as shown by Kiczka et al. (2010) and Moynier et al. (2013), reflecting a varying extent of Fe isotope fractionation during in-plant translocation and redistribution.

5 | CONCLUSION

The present study confirmed our hypothesis that physical pedogenic processes such as clay translocation through leaching did not induce significant Fe isotope fractionation in the studied Albic Luvisol profiles, because this process involves the transport of colloids rather than of dissolved Fe. Long-term liming also did not enforce Fe isotope fractionation processes in the soil, but it led to heavier Fe isotope compositions in winter rye, suggesting that the plants responded to liming by increased Fe uptake through complexation processes. Our finding indicates that the analysis of Fe isotope compositions of field-grown plants is a promising tool for tracing alternations in Fe uptake strategies by plants under changed environmental conditions.

ACKNOWLEDGEMENTS

This work was supported by the German Federal Ministry of Education and Research (BMBF) in the framework of the funding initiative “Soil as a Sustainable Resource for the Bioeconomy – BonaRes”, project “BonaRes (Module A): Sustainable Subsoil Management - Soil³; subproject 3” (grant numbers 031B0026C, 2015). Professor Dr Jan Vanderborght at the Agrosphere Institute at Forschungszentrum Jülich GmbH is acknowledged for the discussion of statistical analyses of the data. We thank the Editor-in-Chief of the European Journal of Soil Science, Professor Jennifer Dungait, and the two anonymous reviewers for their constructive suggestions on this study.

CONFLICT OF INTEREST

We state that the authors have no conflict of interest.

DATA AVAILABILITY STATEMENT

The data of current study will be available at BonaRes Data Portal: <https://datenzentrum.bonares.de/research-data.php>

ORCID

Bei Wu  <https://orcid.org/0000-0003-1784-1992>

Yi Wang  <https://orcid.org/0000-0001-5413-4248>

Sara L. Bauke  <https://orcid.org/0000-0003-2284-9593>

REFERENCES

- Ågren, G. I., & Weih, M. (2012). Plant stoichiometry at different scales: Element concentration patterns reflect environment more than genotype. *New Phytologist*, *194*, 944–952. <https://doi.org/10.1111/j.1469-8137.2012.04114.x>
- Ariga, T., Hazama, K., Yanagisawa, S., & Yoneyama, T. (2014). Chemical forms of iron in xylem sap from graminaceous and non-graminaceous plants. *Soil Science and Plant Nutrition*, *60*, 460–469. <https://doi.org/10.1080/00380768.2014.922406>
- Arnold, T., Markovic, T., Kirk, G.J.D., Schönbacher, M., Rehkämper, M., Zhao, F.J., & Weiss, D.J. (2015). Iron and zinc isotope fractionation during uptake and translocation in rice (*Oryza sativa*) grown in oxic and anoxic soils. *Comptes Rendus Geoscience*, *347*, 397–404. <https://doi.org/10.1016/j.crte.2015.05.005>
- Blume, H.-P., Brümmer, G. W., Fleige, H., Horn, R., Kandeler, E., Kögel-Knabner, I., ... Wilke, B.-M. (2016). *Scheffer/schachtschabel soil science* (1st English ed.). Berlin, Germany. ISBN: 978-3-642-30941-0 (PB), ISBN: 978-3-642-30942-7 (E-Book): Springer-Verlag. <https://doi.org/10.1007/978-3-642-30942-7>
- Bolan, N. S., Adriano, D. C., & Curtin, D. (2003). Soil acidification and liming interactions with nutrient and heavy metal transformation and bioavailability. *Advances in Agronomy*, *78*, 215–272. [https://doi.org/10.1016/S0065-2113\(02\)78006-1](https://doi.org/10.1016/S0065-2113(02)78006-1)
- Briat, J. F. (1999). Plant ferritin and human iron deficiency. *Nature Biotechnology*, *17*, 621. <https://doi.org/10.1038/10797>
- Chen, Y., & Barak, P. (1982). Iron nutrition of plants in calcareous soils. *Advances in Agronomy*, *35*, 217–240. [https://doi.org/10.1016/S0065-2113\(08\)60326-0](https://doi.org/10.1016/S0065-2113(08)60326-0)
- Chmielewski, F.-M., & Köhn, W. (1999). The long-term agrometeorological field experiment at Berlin-Dahlem, Germany. *Agricultural and Forest Meteorology*, *96*, 39–48. [https://doi.org/10.1016/S0168-1923\(99\)00045-3](https://doi.org/10.1016/S0168-1923(99)00045-3)
- Crosby, H. A., Johnson, C. M., Roden, E. E., & Beard, B. L. (2005). Coupled Fe(II)-Fe(III) electron and atom exchange as a mechanism for Fe isotope fractionation during dissimilatory iron oxide reduction. *Environmental Science & Technology*, *39*, 6698–6704. <https://doi.org/10.1021/es0505346>
- Crosby, H. A., Roden, E. E., Johnson, C. M., & Beard, B. L. (2007). The mechanisms of iron isotope fractionation produced during dissimilatory Fe(III) reduction by *Shewanella putrefaciens* and *Geobacter sulfurreducens*. *Geobiology*, *5*, 169–189. <https://doi.org/10.1111/j.1472-4669.2007.00103.x>
- Curie, C., Cassin, G., Couch, D., Divol, F., Higuchi, K., Le Jean, M., ... Mari, S. (2009). Metal movement within the plant: Contribution of nicotianamine and yellow stripe1-like transporters. *Annals of Botany*, *103*, 1–11. <https://doi.org/10.1093/aob/mcn207>
- Dauphas, N., Janney, P. E., Mendybaev, R. A., Wadhwa, M., Richter, F. M., Davis, A. M., ... Foley, C. N. (2004). Chromatographic separation and multicollection-ICPMS analysis of iron. Investigating mass-dependent and -independent isotope effects. *Analytical Chemistry*, *76*, 5855–5863. <https://doi.org/10.1021/ac0497095>

- Dauphas, N., John, S., & Rouxel, O. (2017). Iron isotope systematics. *Reviews in Mineralogy and Geochemistry*, *82*, 415–510. <https://doi.org/10.2138/rmg.2017.82.11>
- Dideriksen, K., Baker, J. A., & Stipp, S. L. S. (2008). Equilibrium Fe isotope fractionation between inorganic aqueous Fe(III) and the siderophore complex, Fe(III)-desferrioxamine B. *Earth and Planetary Science Letters*, *269*, 280–290. <https://doi.org/10.1016/j.epsl.2008.02.022>
- Fageria, N. K., Zimmermann, F. J. P., & Baligar, V. C. (1995). Lime and phosphorus interactions on growth and nutrient uptake by upland rice, wheat, common bean, and corn in an oxisol. *Journal of Plant Nutrition*, *18*, 2519–2532. <https://doi.org/10.1080/01904169509365081>
- Fekiacova, Z., Pichat, S., Cornu, S., & Balesdent, J. (2013). Inferences from the vertical distribution of Fe isotopic compositions on pedogenetic processes in soils. *Geoderma*, *209*, 110–118. <https://doi.org/10.1016/j.geoderma.2013.06.007>
- Fourcroy, P., Sisó-Terraza, P., Sudre, D., Savirón, M., Rey, G., Gaymard, F., ... Briat, J.-F. (2014). Involvement of the ABCG37 transporter in secretion of scopoletin and derivatives by Arabidopsis roots in response to iron deficiency. *New Phytologist*, *201*, 155–167. <https://doi.org/10.1111/nph.12471>
- Grillet, L., Mari, S., & Schmidt, W. (2014). Iron in seeds—Loading pathways and subcellular localization. *Frontiers in Plant Science*, *4*, 535. <https://doi.org/10.3389/fpls.2013.00535>
- Guelke, M., von Blanckenburg, F., Schoenberg, R., Staubwasser, M., & Stuetzel, H. (2010). Determining the stable Fe isotopic signature of plant-available iron in soils. *Chemical Geology*, *277*, 269–280. <https://doi.org/10.1016/j.chemgeo.2010.08.010>
- Guelke-Stelling, M., & von Blanckenburg, F. (2012). Fe isotope fractionation caused by translocation of iron during growth of bean and oat as models of strategy I and II plants. *Plant and Soil*, *352*, 217–231. <https://doi.org/10.1007/s11104-011-0990-9>
- Haynes, R. J., & Naidu, R. (1998). Influence of lime, fertilizer and manure applications on soil organic matter content and soil physical conditions: A review. *Nutrient Cycling in Agroecosystems*, *51*, 123–137. <https://doi.org/10.1023/A:1009738307837>
- Hobley, E. U., & Prater, I. (2019). Estimating soil texture from Vis-NIR spectra. *European Journal of Soil Science*, *70*, 83–95. <https://doi.org/10.1111/ejss.12733>
- Ishimaru, Y., Suzuki, M., Tsukamoto, T., Suzuki, K., Nakazono, M., Kobayashi, T., ... Nishizawa, N. K. (2006). Rice plants take up iron as an Fe³⁺-phytosiderophore and as Fe²⁺. *The Plant Journal*, *45*, 335–346. <https://doi.org/10.1111/j.1365-313X.2005.02624.x>
- IUSS Working Group WRB. (2015). *World reference base for soil resources 2014, update 2015, international soil classification system for naming soils World Soil Resources Report 106*. Rome, Italy: Food and Agriculture Organization of the United Nations.
- Johnson, C. M., Skulan, J. L., Beard, B. L., Sun, H., Nealon, K. H., & Braterman, P. S. (2002). Isotopic fractionation between Fe(III) and Fe(II) in aqueous solutions. *Earth and Planetary Science Letters*, *195*, 141–153. [https://doi.org/10.1016/S0012-821X\(01\)00581-7](https://doi.org/10.1016/S0012-821X(01)00581-7)
- Kappler, A., & Straub, K. L. (2005). Geomicrobiological cycling of iron. *Reviews in Mineralogy and Geochemistry*, *59*, 85–108. <https://doi.org/10.2138/rmg.2005.59.5>
- Kato, M., Ishikawa, S., Inagaki, K., Chiba, K., Hayashi, H., Yanagisawa, S., & Yoneyama, T. (2010). Possible chemical forms of cadmium and varietal differences in cadmium concentrations in the phloem sap of rice plants (*Oryza sativa* L.). *Soil Science and Plant Nutrition*, *56*, 839–847. <https://doi.org/10.1111/j.1747-0765.2010.00514.x>
- Kautz, T., Amelung, W., Ewert, F., Gaiser, T., Horn, R., Jahn, R., ... Köpke, U. (2013). Nutrient acquisition from the arable subsoil in temperate climates: A review. *Soil Biology and Biochemistry*, *57*, 1003–1022. <https://doi.org/10.1016/j.soilbio.2012.09.014>
- Kiczka, M., Wiederhold, J. G., Frommer, J., Voegelin, A., Kraemer, S. M., Bourdon, B., & Kretzschmar, R. (2011). Iron speciation and isotope fractionation during silicate weathering and soil formation in an alpine glacier forefield chronosequence. *Geochimica et Cosmochimica Acta*, *75*, 5559–5573. <https://doi.org/10.1016/j.gca.2011.07.008>
- Kiczka, M., Wiederhold, J. G., Kraemer, S. M., Bourdon, B., & Kretzschmar, R. (2010). Iron isotope fractionation during plant uptake and translocation in alpine plants. *Environmental Science & Technology*, *44*, 6144–6150. <https://doi.org/10.1021/es100863b>
- Krzysz, G., Gaesar, K., Becker, K., Brodowski, M., Dressler, U.-B., Grimm, J., Jancke, G., Krause, S., & Schlenker, L. (1992). Einfluß von langjährig differenzierten Bewirtschaftungsmaßnahmen und Umweltbelastungen auf Bodenfruchtbarkeit und Ertragsleistung eines lehmigen Sandbodens (Influence of long-term differentiated management measures and environmental pollution on soil fertility and yield of a loamy sandy soil). Final Report of the Interdisciplinary Research Project, IFP 15/2, at the Institute of Crop Research, Technische Universität Berlin. Margraf, Berlin, ISSN 0177-6673.
- Liu, C., Gao, T., Liu, Y., Liu, J., Li, F., Chen, Z., ... Huang, W. (2019). Isotopic fingerprints indicate distinct strategies of Fe uptake in rice. *Chemical Geology*, *524*, 323–328. <https://doi.org/10.1016/j.chemgeo.2019.07.002>
- Lotfi-Kalahroodi, E., Pierson-Wickmann, A.-C., Guénet, H., Rouxel, O., Ponzevera, E., Bouhnik-LeCoz, M., ... Davranche, M. (2019). Iron isotope fractionation in iron-organic matter associations: Experimental evidence using filtration and ultrafiltration. *Geochimica et Cosmochimica Acta*, *250*, 98–116. <https://doi.org/10.1016/j.gca.2019.01.036>
- Marschner, H. (1995). *Mineral nutrition of higher plants*. London, England: Academic Press ISBN: 9780124735439 (PB), ISBN: 9780080571874 (Ebook).
- Marschner, H., Römheld, V., & Kissel, M. (1986). Different strategies in higher plants in mobilization and uptake of iron. *Journal of Plant Nutrition*, *9*, 695–713. <https://doi.org/10.1080/01904168609363475>
- Morgan, J. L. L., Wasylenki, L. E., Nuester, J., & Anbar, A. D. (2010). Fe isotope fractionation during equilibration of Fe-organic complexes. *Environmental Science & Technology*, *44*, 6095–6101. <https://doi.org/10.1021/es100906z>
- Mori, S. (1999). Iron acquisition by plants. *Current Opinion in Plant Biology*, *2*, 250–253. [https://doi.org/10.1016/S1369-5266\(99\)80043-0](https://doi.org/10.1016/S1369-5266(99)80043-0)
- Morrissey, J., & Guerinot, M. L. (2009). Iron uptake and transport in plants: The good, the bad, and the ionome. *Chemical Reviews*, *109*, 4553–4567. <https://doi.org/10.1021/cr900112r>
- Moynier, F., Fujii, T., Wang, K., & Fariel, J. (2013). Ab initio calculations of the Fe (II) and Fe (III) isotopic effects in citrates, nicotianamine, and phytosiderophore, and new Fe isotopic

- measurements in higher plants. *Comptes Rendus Geoscience*, 345, 230–240. <https://doi.org/10.1016/j.crte.2013.05.003>
- Nishiyama, R., Kato, M., Nagata, S., Yanagisawa, S., & Yoneyama, T. (2012). Identification of Zn-nicotianamine and Fe-2'-deoxymugineic acid in the phloem sap from rice plants (*Oryza sativa* L.). *Plant and Cell Physiology*, 53, 381–390. <https://doi.org/10.1093/pcp/pcr188>
- Nozoye, T., Nagasaka, S., Kobayashi, T., Takahashi, M., Sato, Y., Uozumi, N., Nakanishi, H. & Nishizawa, N.K. (2011). Phytosiderophore efflux transporters are crucial for iron acquisition in graminaceous plants. *The Journal of Biological Chemistry*, 286, 5446–5454. <https://doi.org/10.1074/jbc.M110.180026>
- OriginLab. (2015). *OriginPro. Release b9.2.272*. Northampton, MA: OriginLab.
- Ravet, K., Touraine, B., Boucherez, J., Briat, J. F., Gaymard, F., & Cellier, F. (2008). Ferritins control interaction between iron homeostasis and oxidative stress in *Arabidopsis*. *The Plant Journal*, 57, 400–412. <https://doi.org/10.1111/j.1365-313X.2008.03698.x>
- Rousseau, M., Di Pietro, L., Angulo-Jaramillo, R., Teissier, D., & Cabidel, B. (2004). Preferential transport of soil colloidal particles: Physicochemical effects on particle mobilization. *Vadose Zone Journal*, 3, 247–261. <https://doi.org/10.2136/vzj2004.2470>
- Ryan, J. N., & Gschwend, P. M. (1998). Effects of ionic strength and flow rate on colloid release: Relating kinetics to intersurface potential energy. *Journal of Colloid and Interface Science*, 164, 21–34. <https://doi.org/10.1006/jcis.1994.1139>
- Schaaf, G., Ludewig, U., Erenoglu, B. E., Mori, S., Kitahara, T., & von Wirén, N. (2004). ZmYS1 functions as a proton-coupled symporter for phytosiderophore- and nicotianamine-chelated metals. *Journal of Biological Chemistry*, 279, 9091–9096. <https://doi.org/10.1074/jbc.M311799200>
- Shojima, S., Nishizawa, N.-K., Fushiya, S., Nozoe, S., Irifune, T., & Mori, S. (1990). Biosynthesis of phytosiderophores. *Plant Physiology*, 93, 1497–1503. <https://doi.org/10.1104/pp.93.4.1497>
- Stomph, J. T., Jiang, W., & Struik, P. C. (2009). Zinc biofortification of cereals: Rice differs from wheat and barley. *Trends in Plant Science*, 14, 123–124. <https://doi.org/10.1016/j.tplants.2009.01.001>
- Vazzola, V., Losa, A., Soave, C., & Murgia, I. (2007). Knockout of frataxin gene causes embryo lethality in *Arabidopsis*. *FEBS Letters*, 581, 667–672. <https://doi.org/10.1016/j.febslet.2007.01.030>
- Walter, K., Don, A., Tiemeyer, B., & Freibauer, A. (2016). Determining soil bulk density for carbon stock calculation: A systematic method comparison. *Soil Science Society of America Journal*, 80, 579–591. <https://doi.org/10.2136/sssaj2015.11.0407>
- Weber, K. A., Achenbach, L. A., & Coates, J. D. (2006). Microorganisms pumping iron: Anaerobic microbial iron oxidation and reduction. *Nature*, 4, 752–764. <https://doi.org/10.1038/nrmicro1490>
- Wiederhold, J. G., Kraemer, S. M., Teutsch, N., Borer, P. M., Halliday, A. N., & Kretzschmar, R. (2006). Iron isotope fractionation during proton-promoted, ligand-controlled, and reductive dissolution of goethite. *Environmental Science & Technology*, 40, 3787–3793. <https://doi.org/10.1021/es052228y>
- Wiederhold, J. G., Teutsch, N., Kraemer, S. M., Halliday, A. N., & Kretzschmar, R. (2007). Iron isotope fractionation in oxic soils by mineral weathering and podzolization. *Geochimica et Cosmochimica Acta*, 71, 5821–5833. <https://doi.org/10.1016/j.gca.2007.07.023>
- Wu, B., Amelung, W., Xing, Y., Bol, R., & Berns, A. E. (2019). Iron cycling and isotope fractionation in terrestrial ecosystems. *Earth-Science Reviews*, 190, 323–352. <https://doi.org/10.1016/j.earscirev.2018.12.012>

SUPPORTING INFORMATION

Additional supporting information may be found online in the Supporting Information section at the end of this article.

How to cite this article: Wu B, Wang Y, Berns AE, et al. Iron isotope fractionation in soil and graminaceous crops after 100 years of liming in the long-term agricultural experimental site at Berlin-Dahlem, Germany. *Eur J Soil Sci*. 2020;1–11. <https://doi.org/10.1111/ejss.12944>